Journal of Hydrology 396 (2011) 1–11

Contents lists available at ScienceDirect

Journal of Hydrology

journal homepage: www.elsevier.com/locate/jhydrol

Field tracer investigation of unsaturated zone flow paths and mechanisms in agricultural soils of northwestern Mississippi, USA

Kim S. Perkins [a,*], John R. Nimmo [a], Claire E. Rose [b], Richard H. Coupe [b]

[a] US Geological Survey, 345 Middlefield Road, Menlo Park, CA 94025, United States
[b] US Geological Survey, 308 South Airport Road, Pearl, MS 39208-6649, United States

ARTICLE INFO

Article history:
Received 16 April 2010
Received in revised form 14 September 2010
Accepted 16 September 2010

This manuscript was handled by Geoff Syme, Editor-in-Chief

Keywords:
Unsaturated zone
Infiltration
Preferential flow
Aquifer recharge
Solute transport
Bromide tracer

SUMMARY

In many farmed areas, intensive application of agricultural chemicals and withdrawal of groundwater for irrigation have led to water quality and supply issues. Unsaturated-zone processes, including preferential flow, play a major role in these effects but are not well understood. In the Bogue Phalia basin, an intensely agricultural area in the Delta region of northwestern Mississippi, the fine-textured soils often exhibit surface ponding and runoff after irrigation and rainfall as well as extensive surface cracking during prolonged dry periods. Fields are typically land-formed to promote surface flow into drainage ditches and streams that feed into larger river ecosystems. Downward flow of water below the root zone is considered minimal; regional groundwater models predict only 5% or less of precipitation recharges the heavily used alluvial aquifer. In this study transport mechanisms within and below the root zone of a fallow soybean field were assessed by performing a 2-m ring infiltration test with tracers and subsurface monitoring instruments. Seven months after tracer application, 48 continuous cores were collected for tracer extraction to define the extent of water movement and quantify preferential flow using a mass-balance approach. Vertical water movement was rapid below the pond indicating the importance of vertical preferential flow paths in the shallow unsaturated zone, especially to depths where agricultural disturbance occurs. Lateral flow of water at shallow depths was extensive and spatially non-uniform, reaching up to 10 m from the pond within 2 months. Within 1 month, the wetting front reached a textural boundary at 4–5 m between the fine-textured soil and sandy alluvium, now a potential capillary barrier which, prior to extensive irrigation withdrawals, was below the water table. Within 10 weeks, tracer was detectable at the water table which is presently about 12 m below land surface. Results indicate that 43% of percolation may be through preferential flow paths and that any water breaking through the capillary barrier (as potential recharge) likely does so in fingers which are difficult to detect with coring methods. In other areas where water levels have declined and soils have similar properties, the potential for transport of agricultural chemicals to the aquifer may be greater than previously assumed.

Published by Elsevier B.V.

1. Introduction

Agricultural practices can impact water quality and water supply by affecting amounts and timing of surface water runoff and groundwater recharge. Irrigation withdrawals have resulted in declining water tables in prolific agricultural areas of the US and around the world (McGuire, 2007; Pimentael et al., 2004; Liu et al., 2001). This potentially has profound effects on the hydrologic influence of the unsaturated zone, particularly in terms of recharge and transport of agricultural chemicals. The Mississippi River Valley alluvial aquifer (hereafter referred to as the alluvial aquifer) underlies the Mississippi embayment, much of which (62–90%) includes intensive row-crop production (Kleiss et al., 2000). Agricultural practices include land-forming to enhance the flow of excess surface water to nearby ditches and streams, and the application of agricultural chemicals. Standing water in fields is common after precipitation as is cracking of the soil surface during prolonged dry periods. It is commonly assumed that the soils have low permeability and infiltration capacity, the effect of which is to minimize percolation below the root zone.

In the Bogue Phalia Basin in northwestern Mississippi (Fig. 1), groundwater withdrawals, primarily for irrigation, have lowered the water table by as much as 10 m. In the central part of the Delta, studies have shown rates of decline of about 0.6 m/y (Crawford, 1990; Sumner and Wasson, 1984; Darden, 1983). The transition from forest to agricultural land was generally accompanied by the use of surface water for irrigation. This practice was discontinued in the early to mid-1990s as stream flows began diminishing.

* Corresponding author. Tel.: +1 650 329 4551; fax: +1 650 329 4538.
E-mail address: kperkins@usgs.gov (K.S. Perkins).

0022-1694/$ - see front matter Published by Elsevier B.V.
doi:10.1016/j.jhydrol.2010.09.009

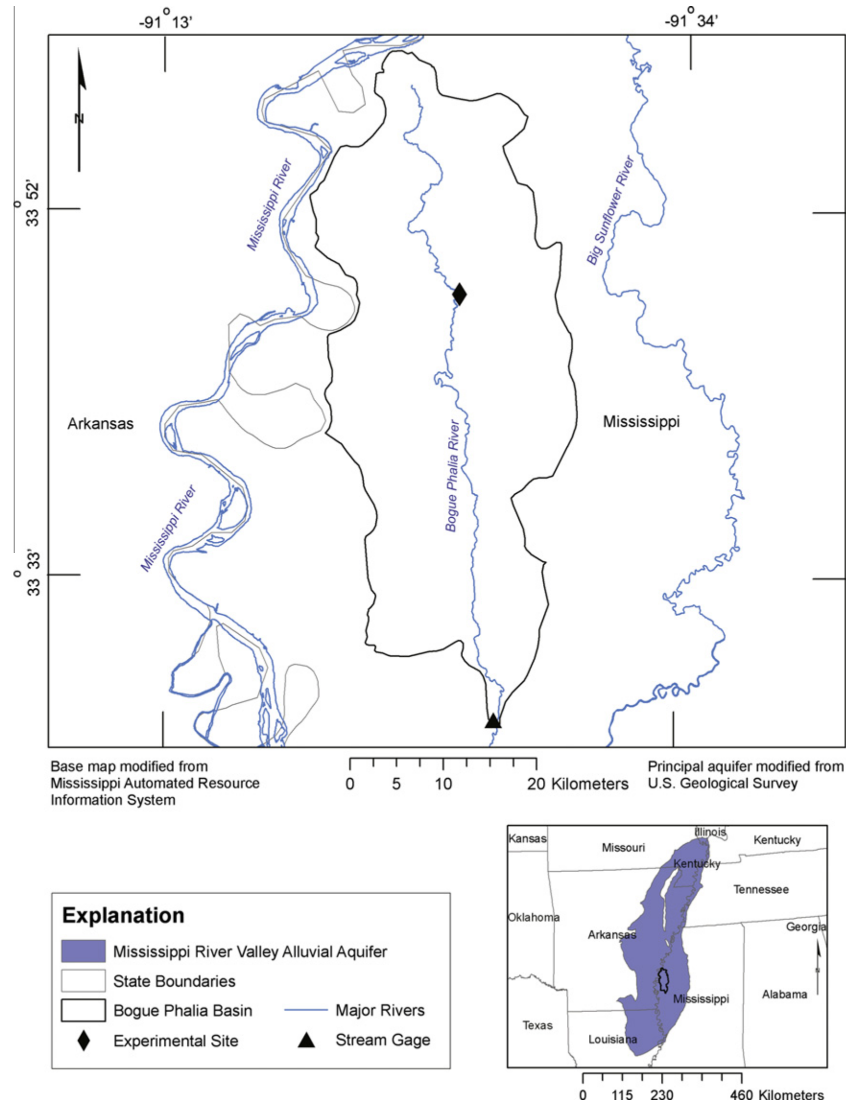

Fig. 1. Map of the extent of the Mississippi Valley Alluvial Aquifer and the experimental site within the Bogue Phalia Basin.

The transition to groundwater use initially reduced the apparent depletion of surface water; however as withdrawals continued and the water table was lowered, stream flows began diminishing again.

Regional groundwater modeling studies by Arthur (2001), which include the Bogue Phalia basin, have suggested that less than 5% of precipitation becomes recharge. Sediment-yield studies conducted within the Delta (Fig. 1) in two watersheds over a 5 year period concluded that precipitation is partitioned about equally into infiltration and runoff (Murphree and Mutchler, 1981). By a simple calculation done for the study presented here, assuming that all of the infiltration is evapotranspired when crops are present and 75% during periods of no canopy, about 12% of the total annual precipitation becomes recharge. By the same analysis, a similar study by Rebich and Knight (2001) suggests that about 12% of precipitation becomes recharge. Tyner et al. (2006) identified long-term preferential flow in field-scale experiments in Tennessee, just north of the Mississippi–Tennessee border, over a 3 year period using a conservative tracer and a mass-balance approach. They estimated that 58% of recharge was due to preferential flow based on bromide losses with values as high as 83% at some locations within the study plot.

While unsaturated flow can occur both through preferential paths and diffusely through the collective pore space of the matrix, the fastest flow will likely occur by preferential flow. The preferential flow definition adopted for this study is water that bypasses a portion of the soil matrix resulting in shorter travel times from the surface to the water table of some fraction of the applied water (Flury et al., 1994). The fastest flow occurring in a hydrologic system can have considerable practical importance, in the context of minimum travel times, if this fast flow transports contaminants in the subsurface. Several studies using bromide tracers in comparable environments have demonstrated the importance of preferential flow through relatively fine-textured agricultural soils (Tyner et al., 2006; Köhne and Gerke, 2005; Jaynes et al., 2001; Yoder, 2001; Iragavarapu et al., 1998). Preferential flow decreases the opportunity for sorption and degradation, which serve as natural remediation mechanisms in soils, by transmitting water quickly to depths where these processes are typically much less effective (Malone et al., 2004; Ray et al., 2004).

The main objective of the study was to provide a better understanding of the fate of infiltrated water, in particular flow through the unsaturated zone, which has implications for the transport of agricultural chemicals to surface and groundwater. This study aimed to: (1) ascertain the fate of water applied during a ponded infiltration test by monitoring soil water and solute movement over a 7 months period, (2) quantify the preferential flow component of infiltration by extracting soil water after a period of 7 months and conducting a mass balance, and (3) examine the possible changes in unsaturated zone hydrology as a result of extensive groundwater withdrawals.

2. Site description

The Bogue Phalia basin (Fig. 1), which receives about 130 cm of precipitation annually (Arthur, 2001), is intensively row-cropped with soybeans, corn, cotton, and sorghum as well as some aquaculture (rice and catfish). The study area was in a 1.5-acre, non-irrigated soybean field located centrally in the Bogue Phalia basin (Fig. 1) near Cleveland, MS. The unsaturated zone consists of a thin, agriculturally disturbed layer in the upper 0.5 m underlain by 4–5 m of subsoil. At a depth of 4–5 m there is a transition to the alluvial sand unit that hosts the aquifer. The primary surficial soil of the region is the Sharkey Series, which is classified as a very-fine, smectitic, thermic Chromic Epiaquert (Natural Resources Conservation Service, 2009); however, measured particle-size distributions show that the soil at and near the study site are silt loam textured, having less clay and more silt than is typical for this soil series. The field is framed by a shallow ditch on the south, a gravel road on the east, residences on the north, and residences and agricultural storage warehouses on the west. The infiltration ring for this field experiment was situated in the southeast corner of the field, with associated instrumentation arranged radially from the ring about 4 m north, east, and west, and about 15 m south towards the ditch (Fig. 2). During the installation of the equipment and the infiltration experiment, the field was fallow. Four months after the experiment soybeans were planted, grew around the experiment at a distance of about 7 m, and were harvested a few weeks before the instrumentation was removed.

The soybean field used in this study has been managed in a consistent manner since 1997. During this time, the field has only been planted in soybeans, and has not been irrigated, tilled, or landformed. The field was not irrigated and glyphosate has been applied as needed, generally three times yearly by a spraying from a ground rig. The landowner reported that 1.5 pints of basic glyphosate was applied to the field before planting in early March, shortly after planting in mid-April, and before cultivating in mid-May.

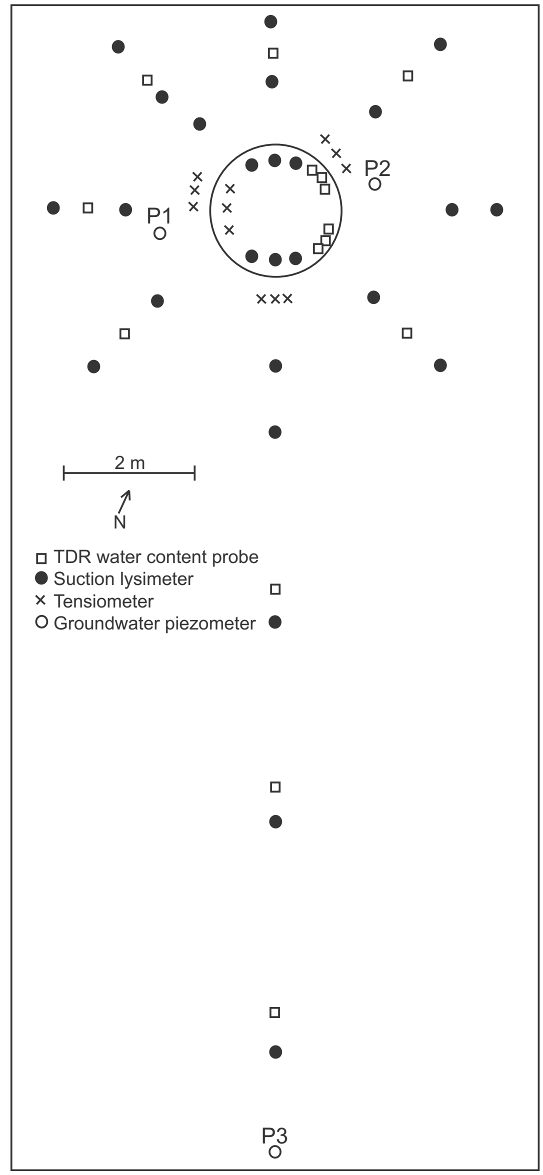

Fig. 2. Map view of the instrumentation layout at the experimental site.

3. Methods

3.1. Preliminary site evaluation

A field method designed to rapidly measure field-saturated hydraulic conductivity (K_{fs}) of soils was used at 42 locations in the Bogue Phalia basin, some of which were near the 2-m ring infiltration site. The sites were chosen based on accessibility and varied in degree of cracking and initial water content. These tests were performed before the 2-m ring infiltration test to assess spatial variability and to guide site selection for the larger-scale infiltration test. The technique uses a portable falling-head, small-diameter, single-ring infiltrometer and an analytical formula for K_{fs} that compensates both for the falling head and for subsurface radial spreading (Nimmo et al., 2009). The infiltrometer, about 28 cm in diameter, was inserted into the ground to a depth of 5–8 cm. Where surface cracking was evident, numerous crack-depth measurements were made and an average value calculated. These tests provided insight in to the spatial and temporal variability of infiltration processes.

3.2. Field experiment

A constant-head ponded infiltration test was conducted in November 2007 with continued subsurface monitoring and sampling through June 2008 with aquifer monitoring continuing until November 2008. A 2-m diameter metal ring was inserted about 5 cm into the soil and sealed around the edges with bentonite to prevent leakage. Tracer-laden water (a total of 1.1 m, 3.45 m^3 in total volume) was added to the ring where the head was held constant near 12 cm for 48 h by means of an automated head-maintaining and data logging device. Once the water supply was shut off, the head dropped for an additional 21 h until the pond was empty. Tracers included rhodamine WT at a nominal concentration of 2.68 kg/m^3, which, due to sorption, served mainly as a visual marker to guide the collection of samples, and calcium bromide at a nominal concentration of 2.37 kg/m^3. Subsurface instruments included time domain reflectometry (TDR) probes to measure water content (θ), tensiometers to measure matric pressure (ψ), suction lysimeters to obtain samples for measuring tracer concentrations, and piezometers to sample for tracer in the saturated-zone and to monitor groundwater water levels with pressure transducers. The water content probes used were Campbell Scientific model CS616 water content reflectometers, which were logged once per minute during the first 2 weeks, then every 15 min throughout the rest of the monitoring period. The tensiometers were installed using a coring tool slightly smaller in diameter than the tensiometer body and porous cup to ensure good contact with the soil and avoid annular flow. The tensiometer data collection scheme was the same as for the TDR probes. The lysimeters were installed with the porous cups dry, suctions of 15–20 psi were applied during samplings. Precipitation data were collected 2.4 km from the site. Subsurface instruments were installed in a radial pattern (Fig. 2). Lysimeters and piezometers were sampled immediately prior to the tracer test to obtain background (native) bromide concentrations. Subsurface probes were logged once per minute. Tracer samples were taken from most lysimeters every 20 min to 2 h for the first 48 h (with the most frequent samplings being closest to the pond), two to three times daily over the following week, and monthly over the following 7 months. The piezometers were sampled daily for the first week, every other month for 5 months, and less frequently through the rest of the year. Samples from the lysimeters and piezometers were analyzed for bromide concentrations using ion chromatography. After 7 months, 48 continuous soil cores were collected (using a Geoprobe, sample diameter of 5 cm) for bromide extraction and analysis: 35 cores to 1-m depth, 10 cores to 5-m depth, 2 cores to 8-m depth, and 1 core directly below the pond to the water table at 12-m depth (Fig. 3). Bromide was extracted from the soil cores using a 10:1 water to dry sediment mixture in order to calculate a mass balance (McMahon et al., 2003).

3.3. Bromide mass calculations

The mass of bromide in the unsaturated zone was computed based on measured concentrations in cells of a 3-dimensional grid imposed on the study area. The mass of bromide in the unsaturated zone, for this study, indicated the mass transported by matrix flow. The difference between that amount and the amount applied to land surface indicated the mass transported by preferential flow. The fraction of infiltrating water that is transported by preferential flow (I_{ref}) was calculated by the tracer budget method of Tyner et al. (2006). Then the preferential flow fraction is defined as

$$I_{pref} = \frac{B_{applied} - B_{soil}}{B_{applied}} \quad (1)$$

where $B_{applied}$ is the mass of the applied bromide and B_{soil} is the total mass of the bromide residing within the volume accessible by diffuse transport. With the experimental site fallow during the study period and the infiltration confined within the 2-m ring, a simplified mass balance could be used to infer preferential flow. The simplifications in the computation included neglecting plant uptake of bromide, plant degradation and soil re-entry of bromide, and loss of bromide in surface runoff which were perceived as unimportant in the particular study due to the controlled field conditions.

Bromide was extracted from three depths within the upper 1 m of soil, and every meter from 1 m depth down to the water table. For estimating B_{soil} from measurements on individual cores, the data from the upper 1 m were of sufficient resolution (93 cores representing a volume of 11.1 m^3) to create contoured volumes from which bromide mass residing in the upper 1 m of soil was calculated. Because the soil core sampling did not establish the maximum lateral extent of diffuse transport in the south and west directions, estimates were based on a maximum possible travel distance of 13 m, which is farther than the tracer was detected in the lysimeter most distant from the pond. For the bromide mass calculation below 1 m depth, data were available from the south transect only (Fig. 3); therefore a specific geometry based on sample location and measured concentrations was assumed to calculate bromide mass. The measured bromide concentrations were assigned to discrete volumes of soil; concentric doughnut shapes of 1-m thickness.

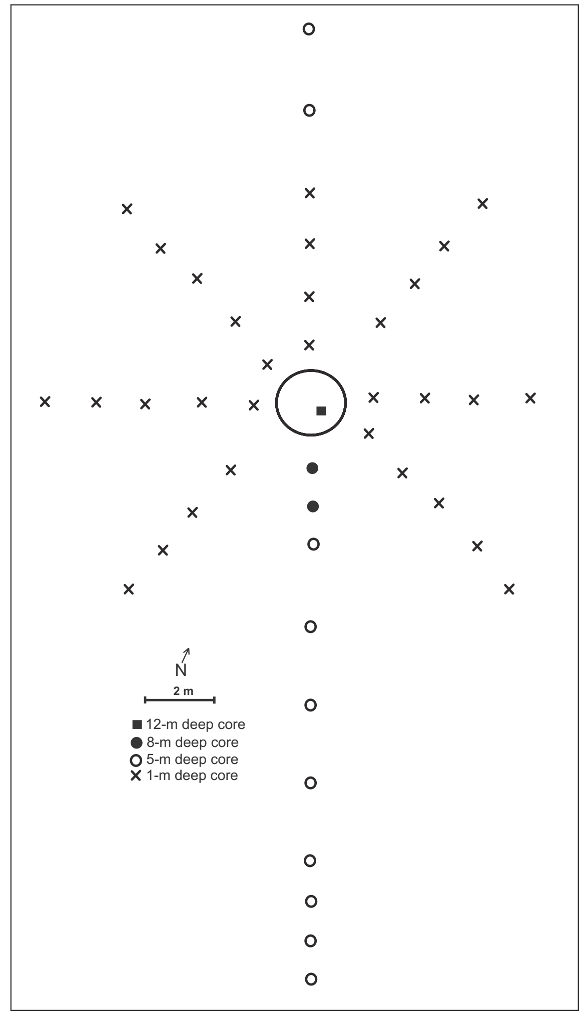

Fig. 3. Map view of continuous core retrieval locations for bromide extraction.

To interpret the mass balance estimation of the preferential fraction of flow, bromide concentrations in aquifer water were used to back-calculate the mass of bromide entering the aquifer from the unsaturated zone between sampling events. This was done using several scenarios represented by different effective volumes of aquifer water that were assumed to dilute the tracer that entered the aquifer. Various dilution scenarios were tested as the effected volume was unknown; volumes selected included a 2-m radius × 1-m thick, a 2-m radius × 2-m thick, a 4-m radius × 2-m thick, and an 8-m radius × 4-m thick cylinder near the top of the aquifer fed by tracer from the unsaturated zone (Fig. 4). The tracer distribution was assumed to be spatially uniform within that volume even though the amount and frequency of tracer leakage to the aquifer was unknown, and very likely could be random due to complex unsaturated-zone processes.

For each aquifer cylinder scenario, the volume of water in each cylinder was calculated by multiplying the volume of the cylinder by an assumed porosity. The estimated tracer mass was calculated by multiplying the average piezometer sample concentrations calculated for each month by the volume of water computed for each

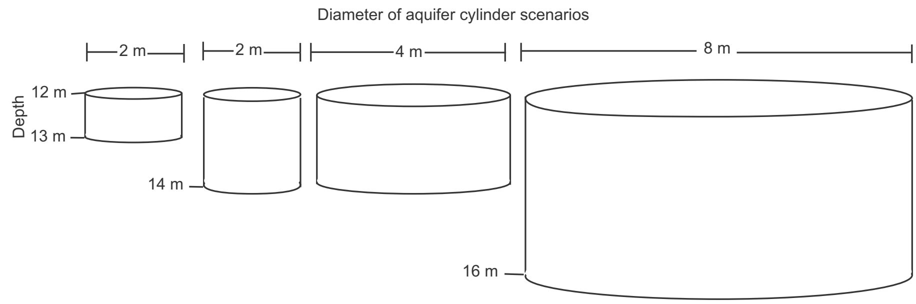

Fig. 4. Depiction of geometry for aquifer cylinder dilution scenarios.

cylinder. The result then is the estimated tracer mass that would reach the aquifer to cause the measured piezometer detection. The aquifer flow rate (0.05 m/day), which was required to determine movement of tracer away from the designated hypothesized volume over time, was calculated using the known local gradient as determined from piezometer water levels (0.025) and the hydraulic conductivity of the aquifer material. The hydraulic conductivity value was 1.9 m/day based on particle size analysis results and from shallow, single-well aquifer tests (Rose, 2007).

The key assumption of the study is that at the time of soil core sampling, tracer transported by preferential flow has moved further from the point of infiltration than would be possible by diffuse (nonpreferential) modes of transport. This requires the core sampling to be extensive enough to include the farthest reaches of diffusely transported tracer, and detailed enough that it supports an estimation of tracer mass throughout the volume affected by diffuse flow.

4. Results

4.1. Hydraulics

For the first 38 min of the constant-head period, the infiltration rate within the pond was 5.6×10^{-5} m/s thereafter remaining steady at 5.2×10^{-6} m/s (Fig. 5). The high initial infiltration rate is caused in part by the low initial saturation state of the shallow soil and filling of shrink-swell cracks and other large macropores beneath the pond. Shallow subsurface transport speeds as inferred from TDR probes and tracer arrivals beneath the pond were highly variable both vertically and laterally, indicative of non-uniform flow (Fig. 6). Because they were logged once per minute, the TDR probe readings more precisely indicated minimum travel time than the lysimeters which were sampled at approximately 45-min to 2-h intervals. In Fig. 6, horizontal bars are shown for each lysimeter to indicate a range of possible values as the tracer arrived at some time between the two samplings. Within 1 month, all instruments down to 60-cm depth had detections (either tracer or water content change), as well as most (70%) instruments down to 120-cm depth. There were no detections at 2.5-m depth; however there was one detection at 5-m depth, 2 m away from the pond in the northeast direction. Within 2 months, all samplers had detections except for the 1-m deep lysimeter 13 m from the pond in the south direction. Bromide was detected in the aquifer 12 m below land surface after 10 weeks. Because bromide was detected at relatively low concentrations, background values were considered in determining the validity of the detections. Background bromide concentrations averaged 3×10^{-4} kg/m^3 with a standard deviation of 9×10^{-5} kg/m^3. Detections considered to be significant were those that were more than three standard deviations above the mean background value (Fig. 7). Of additional importance was the observation of very shallow lateral flow, which may be enhanced by effects of agricultural disturbance near the surface (planting, cultivating, and disking). The soil became wet

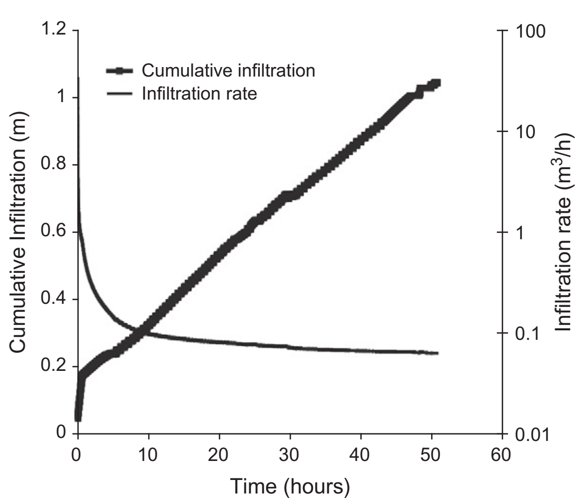

Fig. 5. Plot of cumulative infiltration with respect to time. Small deviations from the overall linear nature of the curve are an artifact of the effort to maintain a constant head during the infiltration test.

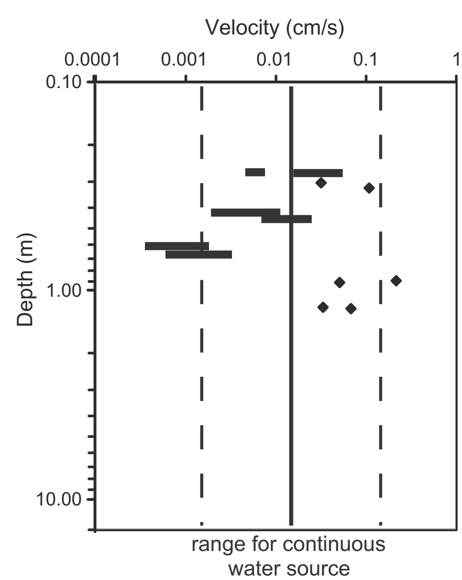

Fig. 6. Plot of minimum travel time of water indicated by TDR probes (diamonds) and suction lysimeters. Lines are shown for each lysimeter to indicate a range of possible values as the tracer arrived at some time between the two samplings. The vertical lines indicate the average and range of values predicted by the Nimmo SRPF model for a continuous water source.

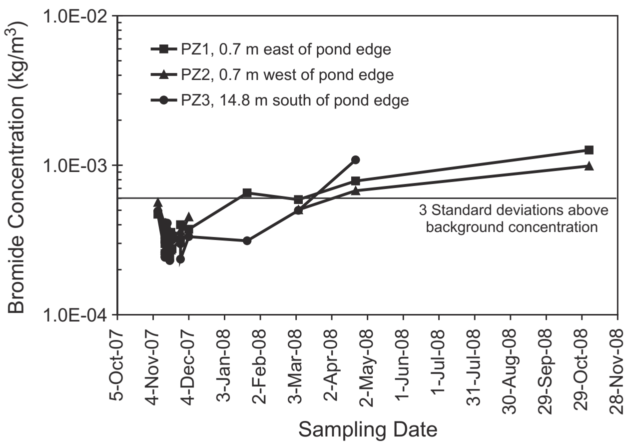

Fig. 7. Bromide concentrations for the aquifer samples showing first arrival after 10 weeks. Piezometer 3 (PZ3) was destroyed following the April 2008 sampling.

at the surface as far as 3–4 m from the pond due to flow in the shallow subsurface which wetted the dry soil above by capillarity.

During the period of study, 79.4 cm of precipitation was measured at the rain gage located 2.4 km from the site.

4.2. Tracer distribution in the unsaturated zone

Bromide concentrations from core extractions were used to evaluate the extent of transport and calculate the mass of bromide remaining in the unsaturated zone 7 months after the infiltration experiment. Data density was sufficient in the upper 1 m (93 samples total from three depths down to 1 m) of soil to create volume contours useful for mass calculations (Fig. 8). The concentrations were calculated using basic volume formulas approximating the basic shape of each contour (cylinder, cube, etc.), each 33-cm thick (Table 1). All calculations below 1 m assumed 10 m maximum diameter radial symmetry (Fig. 9) based data from the south transect (Fig. 3). Tracer was not detected in any core samples below 4.5 m; however, integration of the tracer data was extended down to the water table in order to assess the effect of tracer being present but undetected by the point measurements; the additional mass was found to be negligible (about 30 g total). The calculation of mass below 1 m used measured concentration values assigned to uniform volumes around the measurement points. Table 2 lists the calculated mass of bromide from 1 to 5 m depth. The analysis provides possible values for preferential infiltration.

The sampling domain was bounded by zero bromide concentration values in the horizontal and vertical directions; therefore, it could be assumed that all of the mass within the unsaturated zone was within the sampling domain, although this may not be the case. The textural boundary between the silt loam and sand at 4–5 m likely acts as a capillary barrier, and may cause fingering, as demonstrated by Glass et al. (1989), or other types of preferential flow below 5 m. If finger flow occurred through the sand layer to the water table it would be very difficult to detect using point measurements. Therefore, it is unlikely that all of the tracer mass in the sampling domain is accounted for. Deeks et al. (2008) found, with point samplers, that only 2 of 20 samplers happened to be located in preferential flow paths. For these reasons, conservative assumptions that would tend to underestimate preferential flow contributions were examined.

Calculations based on contour plots result in an estimated 2.2 kg of bromide residing in the upper 1 m of soil (Table 1). Contour lines are dashed where uncertain (Fig. 8). Extending the dashed contours outward as much as 13 m from the pond resulted

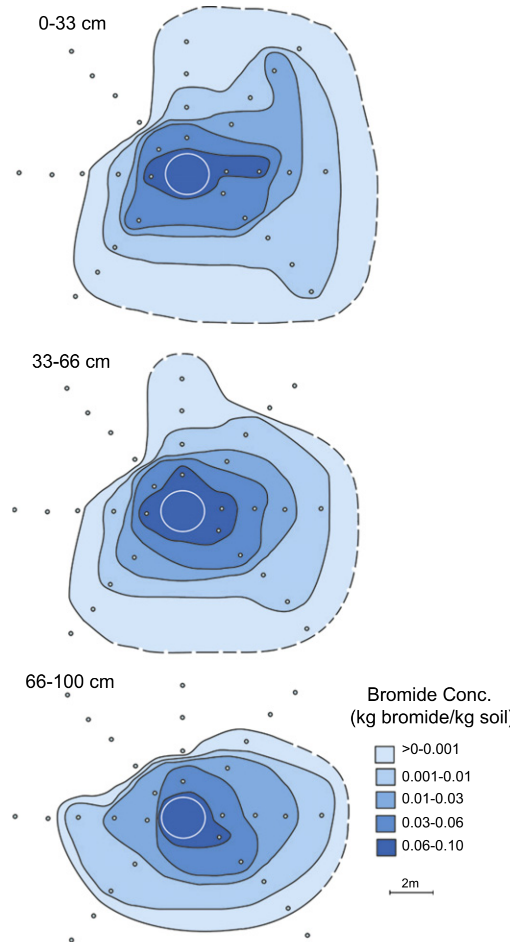

Fig. 8. Bromide concentration contours from the June core sampling for the upper 1 m of soil used in the mass balance calculations. The white ring represents position of the infiltration pond.

Table 1
Bromide mass (kg) calculated for three layers in the upper 1 m of soil based on data from 93 core samples.

Concentration (kg bromide/kg soil)	Bromide mass (kg) for each depth range		
	0–33 cm	33–66 cm	66–100 cm
>0–0.001	0.01	0.03	0.01
0.001–0.01	0.14	0.05	0.06
0.01–0.03	0.04	0.16	0.08
0.03–0.06	0.19	0.30	0.23
0.06–0.10	0.29	0.47	0.16
Total mass for each depth range	0.66	1.00	0.55
Total mass in upper 1 m of soil	2.22		

in little change in mass because the concentrations are so low at these distances from the pond. About 75% of the mass in the upper 1 m of soil is within the two highest concentration contours shown, which are within a few meters of the pond. The mass in the upper 1 m (2.2 kg) was added to the mass calculated below 1 m (2.3 kg, Table 2) and then subtracted from the total amount applied (8.0 kg) to estimate the mass of bromide likely carried by preferential flow beyond the range of sampling. The calculated amount of tracer transported by preferential flow is 43% of the total flow. Bromide is considered a conservative tracer, but if a substantial amount of bromide was absorbed, this estimate of mass

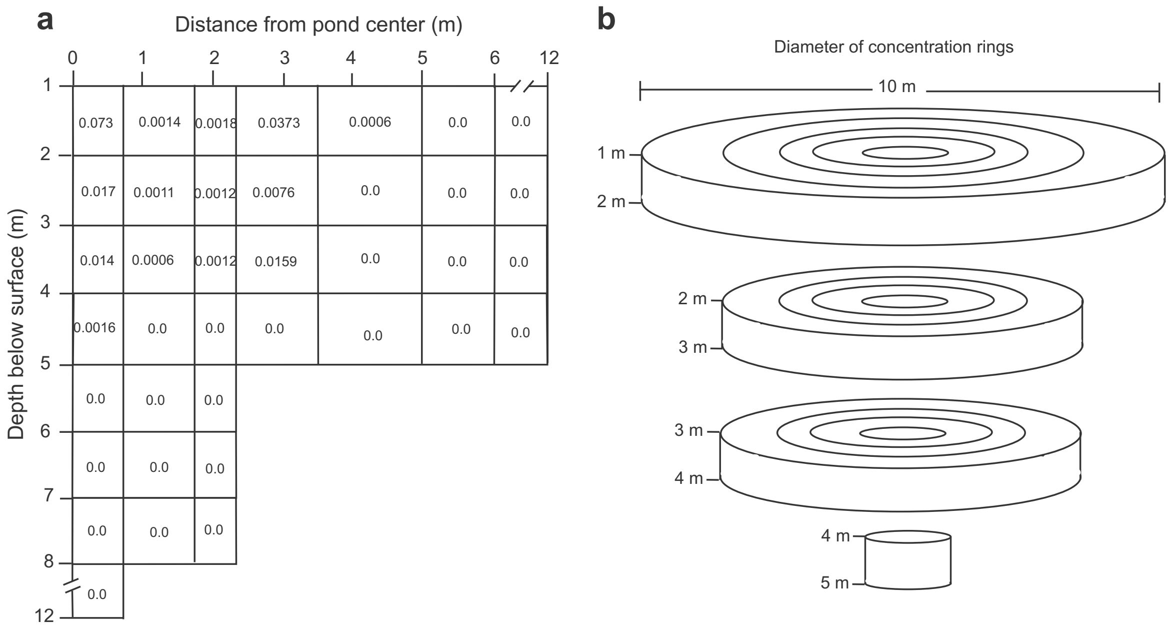

Fig. 9. Bromide concentration data (kg bromide/kg soil) from the June core sampling used in the mass balance calculations for depths below 1 m (a). The concentration data were assigned to volumes based on sample locations and assumed radial symmetry (b). The deepest detection was also extended down to 12 m even though no tracer was detected below 5 m.

Table 2
Bromide mass (kg) calculated for four layers from 1 to 5 m depth based on data from the south sampling transect.

Doughnut lateral dimensions (m, where 0 is center of pond)	Doughnut thickness			
	1–2 m	2–3 m	3–4 m	4–5 m
0–0.75	1.81×10^{-01}	4.30×10^{-02}	3.57×10^{-02}	3.96×10^{-03}
0.75–1.75	1.52×10^{-02}	1.18×10^{-02}	6.59×10^{-03}	0.0
1.75–2.25	1.61×10^{-02}	1.08×10^{-02}	1.09×10^{-02}	0.0
2.25–3.50	1.19	2.42×10^{-01}	5.04×10^{-01}	0.0
3.50–5.00	3.30×10^{-02}	0.0	0.0	0.0
Total mass for each depth range	1.44	3.08×10^{-01}	5.57×10^{-01}	3.96×10^{-03}
Total mass from 1 to 5 m	2.30			

transported by preferential flow would represent an upper limit of the preferential transport fraction.

4.3. Tracer mass in the saturated zone

The piezometer concentration data were used to estimate the amount of tracer moving from the unsaturated zone to the water table in an attempt to reconcile the bromide unaccounted for in the unsaturated-zone mass balance computation. The time range of the tracer mass reaching the water table was known from the piezometer detections, which were interpolated linearly for the months where no data were available due to the limited availability of sampling personnel (Fig. 10). Table 3 lists the monthly bromide concentrations and masses associated with various cylinder dimensions (Fig. 5). The flow rate for the aquifer, 0.05 m/d, implies that for a 2-m diameter cylinder the mass would move out of the zone of tracer addition within 43 days. For a 4-m and 8-m diameter cylinder the times are 86 and 172 days, respectively. Assuming each discrete sampling event represents a monthly pulse of tracer (i.e. using the conservative assumption that all tracer moves out of the area of input within a month), the total mass of bromide added to the aquifer from the first detection through the June core sampling ranges from 0.005 to 0.042 kg (Table 3). From June through the final sample in November, an additional 0.006–0.049 kg reached the aquifer (Table 3).

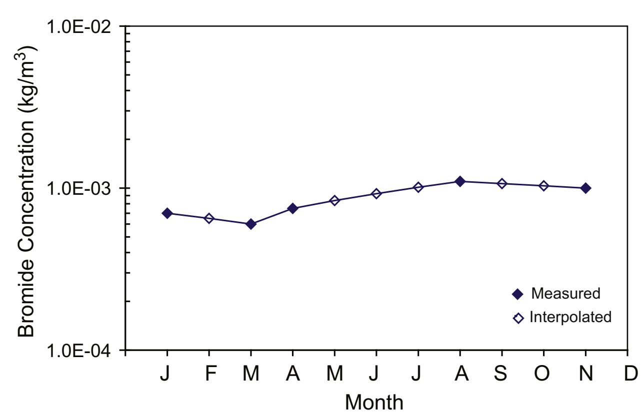

Fig. 10. Bromide concentrations in the alluvial aquifer. Data for the three peizometers were averaged and linearly interpolated between measured points.

4.4. Spatial Variability in the shallow subsurface

The initial small-scale infiltrometer tests were conducted from July 2007 through December 2007. Forty-two tests were completed under a variety of conditions at five field sites, under two

Table 3
Bromide mass reaching the aquifer assuming various cylinder sizes (diameter × height). Asterisks indicate interpolated concentration values.

Month (precipitation)	Bromide mass (kg) for each cylinder scenario				
	Concentration (kg/m^3)	2 × 1 m	2 × 2 m	4 × 2 m	8 × 4 m
January (20.1 cm)	7.00×10^{-04}	8.30×10^{-04}	1.65×10^{-03}	6.59×10^{-03}	5.28×10^{-02}
February* (0.0 cm)	6.50×10^{-04}	7.70×10^{-04}	1.53×10^{-03}	6.12×10^{-03}	4.90×10^{-02}
March (21.3 cm)	6.00×10^{-04}	7.10×10^{-04}	1.42×10^{-03}	5.65×10^{-03}	4.52×10^{-02}
April (12.5 cm)	7.50×10^{-04}	8.90×10^{-04}	1.77×10^{-03}	7.07×10^{-03}	5.65×10^{-02}
May* (0.0 cm)	8.40×10^{-04}	9.90×10^{-04}	1.98×10^{-03}	7.89×10^{-03}	6.31×10^{-02}
June* (26.5 cm)	9.30×10^{-04}	1.09×10^{-03}	2.18×10^{-03}	8.71×10^{-03}	6.97×10^{-02}
July* (6.9 cm)	1.01×10^{-03}	1.19×10^{-03}	2.39×10^{-03}	9.54×10^{-03}	7.63×10^{-02}
August (13.5 cm)	1.10×10^{-03}	1.30×10^{-03}	2.60×10^{-03}	1.04×10^{-02}	8.29×10^{-02}
September* (0.0 cm)	1.17×10^{-03}	1.26×10^{-03}	2.52×10^{-03}	1.01×10^{-02}	8.04×10^{-02}
October* (0.0 cm)	1.03×10^{-03}	1.22×10^{-03}	2.44×10^{-03}	9.73×10^{-03}	7.79×10^{-02}
November (27.0 cm)	1.00×10^{-03}	1.18×10^{-03}	2.36×10^{-03}	9.42×10^{-03}	7.54×10^{-02}
Total mass added through June (kg)	5.27×10^{-03}	5.27×10^{-03}	1.05×10^{-02}	4.20×10^{-02}	
Total mass added June–November (kg)	6.15×10^{-03}	6.15×10^{-03}	1.23×10^{-02}	4.91×10^{-02}	

crop types, and different agricultural management practices. The measured K_{fs} values varied over more than four orders of magnitude, from 1.6×10^{-1} to 9.3×10^{-6} cm/s. The K_{fs} values vary over time, and the range in measured values is influenced by agricultural management practices, antecedent soil moisture conditions, and spatial soil heterogeneity.

Table 4 gives the average of hydraulic conductivity measurements made with infiltrometers for each field site and illustrates how the differences in agricultural management practices can affect the infiltration capacity. For example, Pace-I and Pace-NI sites are within 1.6 km of each other and are both soybean fields; however, Pace-I is irrigated and Pace-NI is not. Infiltrometer tests were done during the same seasons, yet the average K_{fs} for all tests run at Pace-NI is higher (1.9×10^{-2} cm/s) than the average of K_{fs} for all tests run at Pace-I (4.7×10^{-4} cm/s). Without irrigation to keep the soil moist, the Pace-NI site probably developed more substantial macropores, as shrinkage cracks, than Pace-I site. Multiple tests were conducted on the Pace-NI field on four separate occasions: early September, mid-September, early October, and mid-December. The K_{fs} values were averaged by date (Fig. 11). The early September tests were conducted soon after harvest and disking. Because lateral flow throughout the disked layer is probable, the September average K_{fs} at the Pace-NI site was higher than at any other time (4.3×10^{-2} cm/s). This higher K_{fs} also may be attributed, in part, to the presence of larger or more numerous macropores within the disked layer compared to those at the Pace-I site due to lack of irrigation, which would limit swelling potential. In mid-September, when surface soil cracks were 1.3 cm deep on average, the average infiltration capacity was 5.6×10^{-3} cm/s. This was lower than in early September 2007. This change of K_{fs} likely is caused by the settling of surface soil after disking. By mid-December, the average K_{fs} of the field was lower than in mid-September, at 5.4×10^{-4} cm/s, despite 0.3 cm cracks at the surface; the prolonged wet conditions of the winter season likely contributed to the reduction of macropores at and near the soil surface.

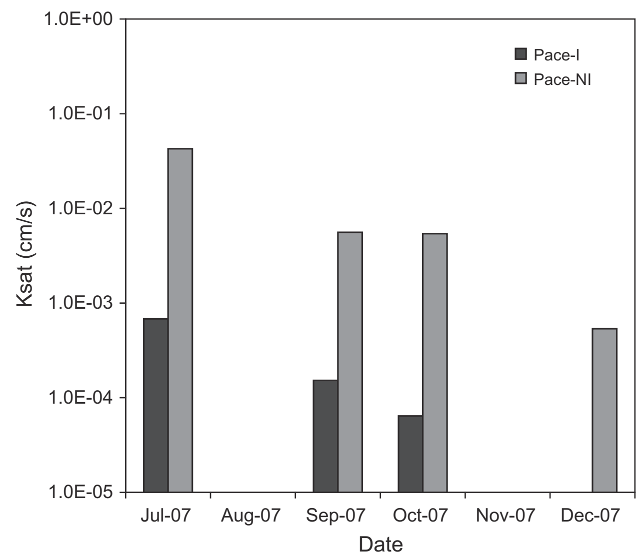

Fig. 11. Saturated hydraulic conductivity values averaged for each measurement date.

5. Discussion

Evidence for preferential flow includes the variability of minimum travel times below the pond (Fig. 6), detection of bromide at depths of 5 m prior to detection at 2 m, spatially variable bromide concentrations below 1 m (Fig. 9), and piezometer detections of bromide in groundwater with no detections in the unsaturated zone below 5 m depth (Fig. 7). For comparison, the Nimmo (2007) Source-Responsive Preferential-Flow (SRPF) travel-time model was used to estimate minimum travel time from the land surface to the aquifer. As the dominant influence on travel times,

Table 4
Average initial K_{fs}, field conditions, and precipitation data for small-scale infiltrometer tests in Pace, MS.

Field site	Date	Average K_{fs}/standard deviation (cm/s)	Field condition	Precipitation since last test (cm)
Pace-I	07/10/07	$6.8 \times 10^{-4}/1.1 \times 10^{-3}$	Before harvest	–
Pace-I	09/05/07	$1.5 \times 10^{-4}/5.1 \times 10^{-5}$	Before harvest	0.3
Pace-I	10/10/07	$6.4 \times 10^{-5}/7.4 \times 10^{-5}$	Harvest and disk 10/4; not smoothed	7.1
Pace-NI	09/05/07	$4.3 \times 10^{-2}/5.3 \times 10^{-2}$	After harvest and disking	–
Pace-NI	09/18/07	$5.6 \times 10^{-3}/4.2 \times 10^{-4}$	1.3 cm cracks at surface	5.3
Pace-NI	10/04/07	$5.4 \times 10^{-3}/4.1 \times 10^{-3}$	No information	1.8
Pace-NI	12/18/07	$5.4 \times 10^{-4}/5.7 \times 10^{-4}$	0.3 cm cracks at Surface	12.7

this model emphasizes the temporal nature of water supply that drives flow along preferential paths. With the assumption that preferential flow is the dominant mode of travel, the model can provide an order-of-magnitude estimate of the fastest travel times. The model makes a strong distinction between cases where this water supply is (1) continuous, as is common in Mississippi rice fields, irrigation ditches, and areas of persistent standing water; and (2) intermittent, such as immediate infiltration of rainfall. A simple formula is applied for continuous cases, and a modified version of that formula to intermittent cases. The value of this approach is supported by collective evaluation of numerous case studies (Nimmo, 2007), in which fastest travel times correlate strongly with the nature of the water supply but not with the particular earth materials involved.

Two possible flow scenarios for the Mississippi soil were examined by applying the SRPF model. In one scenario, if preferential flow was vertical all the way to the water table driven solely by water infiltrated during the experiment, the maximum velocity predicted by the SRPF model is 1 day. This rate is much faster than the bromide tracer was detected in any of the deep lysimeters or piezometers. It is, however, consistent with the timing of the shallow tracer detections suggesting that such flow was driven solely by the infiltration event (Fig. 6). The second, and seemingly more realistic scenario in terms of water flow to the aquifer, considers that some of the infiltration is not vertically downward, but initially spreads laterally (as observed) and subsequently driven downward to the water table in response to intermittent precipitation (79.4 cm of precipitation fell during the period of study) with start-and-stop preferential flow. In this scenario, the model predicts a travel time of about 6 months. This rate is 2.4 times slower than travel times of the measured detections of bromide at the water table, but within the model's factor-of-10 expectation of accuracy. This analysis suggests that most recharge to the aquifer does not move through the unsaturated zone on the timescale of individual infiltration events but rather as the collective result of infiltration over a few months or years.

The mass balance results along with the aquifer dilution calculations indicate that much of the tracer was still residing in the unsaturated zone (as much as 3.5 kg of the 8.0 kg added to the system) at the time the core samples were taken and through the end of the monitoring period (approximately a year after the tracer application). From the first detection of bromide in the aquifer through the June core sampling the mass of tracer added to the aquifer was less than 42 g. This suggests that 40–43% of the amount of bromide mass was still residing in or in the matrix adjacent to preferential flow paths within the unsaturated zone after 7 months. By the last sampling in November, aquifer concentrations were still rising and an additional 6–49 g of tracer may have entered the aquifer, suggesting between 35% and 43% of the bromide mass remained in the unsaturated zone, possibly within isolated zones of high concentration that were underrepresented in the core sampling.

Because the hydrology of the unsaturated zone at this site has changed dramatically since the time forests were cleared for agriculture and surface and groundwater were used for irrigation, it is critical to consider the past and present conditions to understand the implication of a lower water table on aquifer recharge and agricultural chemical transport . The observation of rapid vertical flow and shallow lateral flow in the root zone is useful in reconstructing past conditions. As the top 1 m of soil has undergone little change in agricultural practices over time, it may be assumed that shallow processes have remained stable over this relatively short time period.

Based on the available data and observations, two conceptual models are considered. Fig. 12a depicts a conceptual model representing the higher water table that existed until the mid-1990s before substantial declines occurred as a result of withdrawals for irrigation and other purposes. Prior to these withdrawals, water would have reached the aquifer rapidly, possibly causing a substantial water level rise during large storms. The water would have been mostly diverted into irrigation ditches and streams through lateral flow within the shallow soils, as observed during the experiment, as well as near the surface of the water table with the prevailing groundwater flow direction (aquifer water was discharging to streams prior to widespread groundwater withdrawals). Fig. 12b depicts a plausible conceptual model of unsaturated zone water movement at the present water table depth. Detections of bromide in the unsaturated zone and at the water table provide evidence of preferential flow mechanisms that are important given the current thickness of the unsaturated zone. Lateral flow occurs in the shallow soil layer as observed and is likely at the principal textural boundary at the 4–5 m depth. Flow into the alluvial sand may proceed by fingering or other preferential flow mechanisms to reach the aquifer. If the model of Fig. 12b reasonably represents actual field conditions, there is greater potential impact on unsaturated-zone and aquifer water quality than there was in earlier periods when the water table was higher; subsurface water quality is more vulnerable to degradation as less infiltration makes its way directly to ditches or streams. Under the lower water table condition, infiltrated water may reach the aquifer rapidly through preferential flow paths or temporarily reside in unsaturated zone storage, as inferred from the results of aquifer dilution calculations, until subsequent infiltration initiates movement to the aquifer.

Simplifying assumptions and measurement uncertainties in this study impose cautions in applying its results. (1) The assumed radial symmetry of tracer distribution deviates from the actual distribution. Measurements in the upper meter of soil indicate some degree of symmetry. However, due to the availability of data in only one direction for the deeper samples, it is not known how much of this symmetry persists as tracer is carried deeper. This uncertainty implies a possible over- or underestimation of mass below 1 m depth as there might be higher or lower concentrations existing in other radial directions. (2) The core samples represent a very small volume relative to the volume of tracer-containing soil, which could lead to significant over- or underestimation of the mass of bromide remaining in the unsaturated zone. (3) For the dilution calculations, the estimated saturated-zone flux away from the measurement zone was based on measured bromide concentrations and the known local hydraulic gradient with the assumption of discrete volumes of water moving away on an approximately monthly basis. This assumption could underestimate the bromide mass entering the aquifer under the more likely scenario that bromide enters the aquifer more steadily between calculation periods. However, the measured aquifer concentrations are quite small and even if increased by an order of magnitude, the mass would still only be on the order of a few hundred grams, not enough to significantly decrease the calculated mass assumed to reside in the unsaturated zone. (4) The random instrument error in the bromide concentration measurements (determined from duplicate samples) may be as much as 20%, which would also influence the calculated masses (either increasing or decreasing). All of these factors considered, the calculated masses could be higher or lower in the unsaturated zone and the aquifer, but the magnitude of discrepancy would not influence the basic interpretation of the importance of preferential flow in agricultural environments and the probable effects of groundwater depletion.

Of additional importance is the effect of the mode of water application on preferential flow. Several studies have found more pronounced preferential flow under ponded conditions than under sprinkling (Flury et al., 1994; Ghodrati and Jury, 1990); however, another comparative study by Ghodrati and Jury (1992) showed that the method of water application had no effect on pesticide

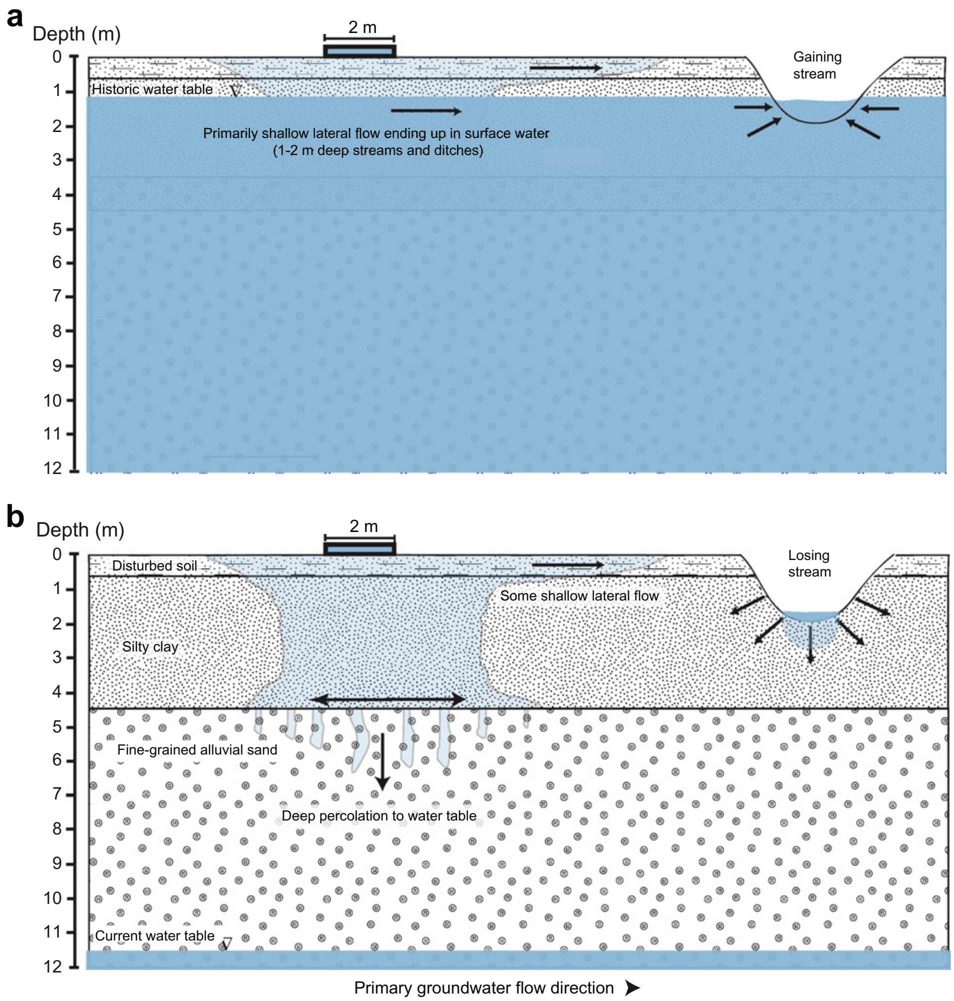

Fig. 12. Conceptual models of flow through the unsaturated zone with the historic water table (a) and the current configuration of the water table (b).

transport. In this study, ponding may have activated preferential flow paths that would not be active under natural rainfall; however, much of the water movement occurred in the days and weeks after the experiment suggesting that rainfall subsequently drove the tracer downward to the water table in response to intermittent precipitation (79.4 cm of precipitation fell during the period of study) with start-and-stop preferential flow.

The results of this study have practical implications for similar agricultural areas. Groundwater depletion can lead to a hydraulically significant thickening of the unsaturated zone, where flow processes are complex and highly nonlinear. This has a direct effect on the variety of mechanisms for solute movement, some possibly allowing faster movement, such as preferential flow, and some that may retard movement allowing degradation of contaminants, such as increased storage time in the unsaturated zone. Possibly altered proportions of vertical to lateral flow may reduce the threat of surface water contamination and increase the threat of agricultural chemicals in groundwater. For the Mississippi study site, glyphosate, which has an average half-life of about 50 days, is the main contaminant of interest. Increased residence time in the unsaturated zone could be a positive effect of a lower water table, allowing degradation of much of the chemical mass rather than fast travel to surface water ecosystems where aquatic organisms might be affected. For contaminants having longer half-lives, preferential flow may increase the likelihood of persistent contamination to aquifer resources.

6. Conclusions

Infiltration rates from a series of small-scale infiltration tests and with a 2-m diameter infiltration ring were higher than expected based on prevailing concepts of low regional infiltration rates and recharge. Measured K_{fs} values within the Bogue Phalia basin vary more than four orders of magnitude from 1×10^{-1} to 9×10^{-6} cm/s. Hydraulic conductivity was shown to vary spatially within an agricultural field and temporally due to soil moisture conditions and agricultural management practices. The relatively high infiltration rates are attributed in part to shallow lateral spreading and preferential flow. In the 2-m ring test water movement was detected below the root zone in less than an hour and lateral flow was non-uniform and extensive at shallow depths. There are multiple lines of evidence for preferential flow including detection of bromide at a depth of 5 m prior to detection at 2 m, spatially variable bromide concentrations below 1 m, and detections of bromide in the aquifer but not in the deep unsaturated zone. Core samples were taken to calculate a mass balance, where about 43% of the infiltrated bromide was missing from the sampled volume, also indicative of preferential flow which is difficult to capture in point measurements. A boundary between silt loam soil and alluvial sand at 4–5 m depth promotes lateral flow and may lead to fingered flow into underlying sand. Based on measured aquifer concentrations over time, it is likely that much of the applied bromide mass was still residing in the unsaturated zone, possibly in isolated flow paths, as much as a year after application. Lowering of the water table over the past couple of decades probably has decreased the likelihood of infiltrated water being transported laterally in the shallow subsurface to nearby streams and ditches, but may have led to deeper transport and greater quantities of agricultural chemicals reaching the aquifer and residing in unsaturated zone storage where degradation may occur.

Acknowledgements

The authors would like to acknowledge the hard work of many who made this study possible: Patrick Mills, Michael Manning, Allen Roberts, Heather Welch, Bobby Richards, Hunter Berch, Jared Smith, Tammy McKaskle, Trent Snellings, and Rick Healy. The authors are grateful for the thoughtful reviews provided by Randall Bayless and Patrick Mills. Funding for this work was provided by the USGS National Water Quality Assessment Program.

References

Arthur, J.K., 2001. Hydrogeology, model description, and flow analysis of the Mississippi River alluvial aquifer in northwestern Mississippi. USGS Water-Resour. Invest. Rept., 01–4035.

Crawford, J.L. 1990. Potentiometric surface of the Mississippi River valley alluvial aquifer, 1981–1989. Proceedings, Twentieth Mississippi Water Resources Conference, April 10–11, 1990. Jackson, MS. Water Resour. Res. Inst., MS. State Univ., 39762, 147–155.

Darden, D., 1983. Water-level maps of the Mississippi alluvial aquifer, northwestern Mississippi, September 1982. USGS Water Resour. Invest. Rept., 83–4133.

Deeks, L.K., Bengough, A.G., Stutter, M.I., Young, I.M., Zhang, X.X., 2008. Characterisation of flow paths and saturated conductivity in a soil block in relation to chloride breakthrough. J. Hydol. 348, 431–441.

Flury, M., Flüler, H., Jury, W.A., Leuenberger, J., 1994. Susceptibility of soils to preferential flow of water: a field study. Water Resour. Res. 30, 1945–1954.

Ghodrati, M., Jury, W.A., 1990. A field study using dyes to characterize preferential flow of water. Soil Sci. Soc. Am. J. 54, 1558–1563.

Ghodrati, M., Jury, W.A., 1992. A field study of the effects of soil structure and irrigation method on preferential flow of pesticides in unsaturated soil. J. Contam. Hydrol. 11, 101–125.

Glass, R.J., Steenhuis, T.S., Parlange, J.-Y., 1989. Wetting front instability 2. Experimental determination of relationships between system parameters and two-dimensional unstable flow field behavior in initially dry porous media. Water Resour. Res. 25, 1207–7795.

Iragavarapu, T.K., Posner, J.L., Bubenzer, G.D., 1998. The effect of various crops on bromide leaching to shallow groundwater under natural rainfall conditions. J. Soil Water Conserv. 53, 146–151.

Jaynes, D.B., Ahmed, S.I., Kung, K.J.S., Kanwar, R.S., 2001. Temporal dynamic of preferential flow to a subsurface drain. Soil Sci. Soc. Am. J. 65, 1368–1376.

Kleiss, B.A., Coupe, R.H., Gonthier, G.J., Justus, B.J. 2000. Water Quality in the Mississippi Embayment, Mississippi, Louisiana, Arkansas, Missouri, Tennessee, and Kentucky, 1995–1998. USGS Circular 1208.

Köhne, J.M., Gerke, H.M., 2005. Spatial and temporal dynamics of preferential bromide movement towards a tile drain. Vadose Zone J. 4, 78–88.

Liu, C., Yu, J., Kendy, E., 2001. Groundwater exploitation and its impact on the environment in the North China Plain. Water Int. 26, 265–272.

McMahon, P.B., Dennehy, K.F., Michel, R.L., Sophocleous, M.A., Ellett, K.M., Hurlbut, D.B., 2003. Water movement through thick unsaturated zones overlying the central High Plains aquifer, southwestern Kansas, 2000–2001. USGS Water Resour. Invest. Rept., 2003–4171.

Malone, R.W., Shipitalo, M.J., Meek, D.W., 2004. Relationship between herbicide concentrations in percolate, percolate breakthrough time, and number of active macropores. Trans. ASAE. 43, 1453–1456.

McGuire, V.L., 2007. Changes in water levels and storage in the high plains aquifer, predevelopment to 2005. USGS Fact Sheet 2007, 3029.

Murphree, C.E., Mutchler, C.K., 1981. Sediment yield from a flatland watershed. Trans. ASAE 24, 966–969.

Natural Resources Conservation Service, Web Soil Survey, 2009: NRCS data available on the web. <http://websoilsurvey.nrcs.usda.gov/app/WebSoilSurvey.aspx> (accessed August 2009).

Nimmo, J.R., 2007. Simple predictions of maximum transport rate in unsaturated soil and rock. Water Resour. Res. 43, 5.

Nimmo, J.R., Schmidt, K.M., Perkins, K.S., Stock, J.D., 2009. Rapid measurement of field-saturated hydraulic conductivity for areal characterization. Vadose Zone J. 8, 142–149.

Pimentael, D., Berger, B., Filiberto, D., Newton, M., Wolfe, B., Karabinakis, E., Clarke, S., Poon, E., Abbett, E., Nanadagopal, S., 2004. Water resources: agricultural and environmental issues. BioSci. 54, 909–918.

Ray, C., Vogel, T., Duesk, J., 2004. Modeling depth-variant and domain-specific sorption and biodegradation in dual-permeability media. J. Contam. Hydrol. 70, 63–87.

Rebich, R.A., Knight, S., 2001. The Mississippi delta management systems evaluation areas project, 1995–99. Miss. Agric. Forest. Exp. Sta. Info. Bull. 377, 154–168.

Rose, C.E. 2007. Determining potential for direct recharge in the Mississippi River Valley alluvial aquifer using soil core analyses, Washington County, northwestern Mississippi. MS Water Resour. Res. Inst. <http://www.wrri.msstate.edu/pdf/rose07.pdf>.

Sumner, D.M., Wasson, B.E., 1984. Summary of results of an investigation to define the geohydrology and simulate the effects of large groundwater withdrawals on the Mississippi River alluvial aquifer in northwestern Mississippi. USGS Water Resour. Invest. Rept., 84–4343.

Tyner, J.S., Wright, W.C., Yoder, R.E., 2006. Identifying long-term preferential and matrix flow recharge at the field scale. Trans. ASABE 50, 2001–2006.

Yoder, R.E. 2001. Field-scale preferential flow at textural discontinuities. In: Proceedings 2nd International Symposium of Preferential Flow, St Joseph, Mich. ASAE, 65–68.